

Eulerian Mean Sea-Surface Velocity Field of the South Indian Ocean Derived by Combining Satellite Altimeter and Drifter Data

Peter, Benny. N
Cochin University of Science and Technology, India

Ambe, Daisuke
National Research Institute of Fisheries Science, Japan

Imawaki, Shiro
Research Institute for Applied Mechanics, Kyushu University | Japan Agency for Marine-Earth Science and Technology, Japan

Peter, Benny N
Cochin University of Science and Technology, India

<https://doi.org/10.15017/14182>

出版情報：九州大学応用力学研究所所報. 135, pp.37-44, 2008-09. Research Institute for Applied Mechanics, Kyushu University

バージョン：

権利関係：



Eulerian Mean Sea-Surface Velocity Field of the South Indian Ocean Derived by Combining Satellite Altimeter and Drifter Data

Benny N. PETER^{*1}, Daisuke AMBE^{*2} and Shiro IMAWAKI^{*3}

E-mail of corresponding author: *bennypeter@gmail.com*

(Received July 31, 2008)

Abstract

Eulerian mean velocity field of south Indian Ocean is estimated with a resolution of 1/3 x 1/3 degree in latitude and longitude by combining satellite altimeter and surface drifting buoy observations. High resolution maps of sea level anomaly (merged T/P or JASON and ERS1/2 or Envisat) and the surface drifter data from the Global Drifter Program during 1993 January - 2004 January have been utilized. Mean winds fields measured by scatterometers onboard ERS/Quikscat is used for computing the wind-driven Ekman current. The estimated mean velocity field illustrates strong boundary currents, zonal currents and weak flows prevail at the central part. The Agulhas Current velocity even reaches 2 m/s at around 35°S. The estimated field tends to be smaller than simple averages of drifter-derived velocities for both the boundary currents and the zonal flow, where the anomaly field dominates. Comparison of the instantaneous velocity field estimated using the mean field and the available Acoustic Doppler Current Profilers depict better correlation.

Key words : *Currents, Circulation, Altimetry, Drifter, South Indian Ocean*

1. Introduction

The south Indian Ocean is a dynamically very active region that houses strong western boundary currents such as Agulhas Current, East Madagascar Current, Mozambique Current and also the seasonally reversing eastern boundary South Java Current and the seasonal Leeuwin Current, besides the equatorial currents. These currents are supposed to be key links in the climatically important global thermohaline circulation by exchanging tropical surface and thermocline waters.

The south Indian Ocean does not experience the monsoonal winds and hence, the seasonal circulation is not as variable as in the north Indian Ocean. Many facts on its surface circulation are not yet completely accomplished. Most of the available information is based on the ship drifts and occasional current meter deployments. The hydrographic sections at selected

locations give the relative flow field referred to some arbitrary levels.

A preliminary information on currents of the south Indian Ocean using hydrographic observations was given by Wyrtki(1973)¹⁾. Later, Reverdin et al. (1983)²⁾, Shetye and Michael (1988)³⁾, Molinari et al. (1990)⁴⁾ and Shenoi et al. (1999)⁵⁾ used the drifting buoy data to study the currents here. Benny and Mizuno (2000)⁶⁾ derived the surface circulation of the tropical Indian Ocean from temperature profiles. Employing the historical hydrographical observations, Reid (2003)⁷⁾ gave a description of the Indian Ocean circulation. Woodberry et al. (1989)⁸⁾ and Kindle and Thompson (1989)⁹⁾ performed numerical modelling studies to simulate the large-scale upper ocean circulation.

Much attention has been given to study the regional circulation in the western and eastern parts of the south Indian Ocean. Grundlingh et al. (1997)¹⁰⁾ and Stramma and Lutjeharms (1997)¹¹⁾ portrayed the upper ocean circulation of the southwest Indian Ocean. Bryden and Beal (2001)¹²⁾ detailed the transport and meridional exchanges of the Agulhas Current.

The poleward flow of the Leeuwin Current against the prevailing wind in the eastern part of the south

*1 Cochin University of Science and Technology, India

*2 National Research Institute of Fisheries Science, Japan

*3 Research Institute for Applied Mechanics, Kyushu University; Present affiliation: Japan Agency for Marine-Earth Science and Technology, Japan

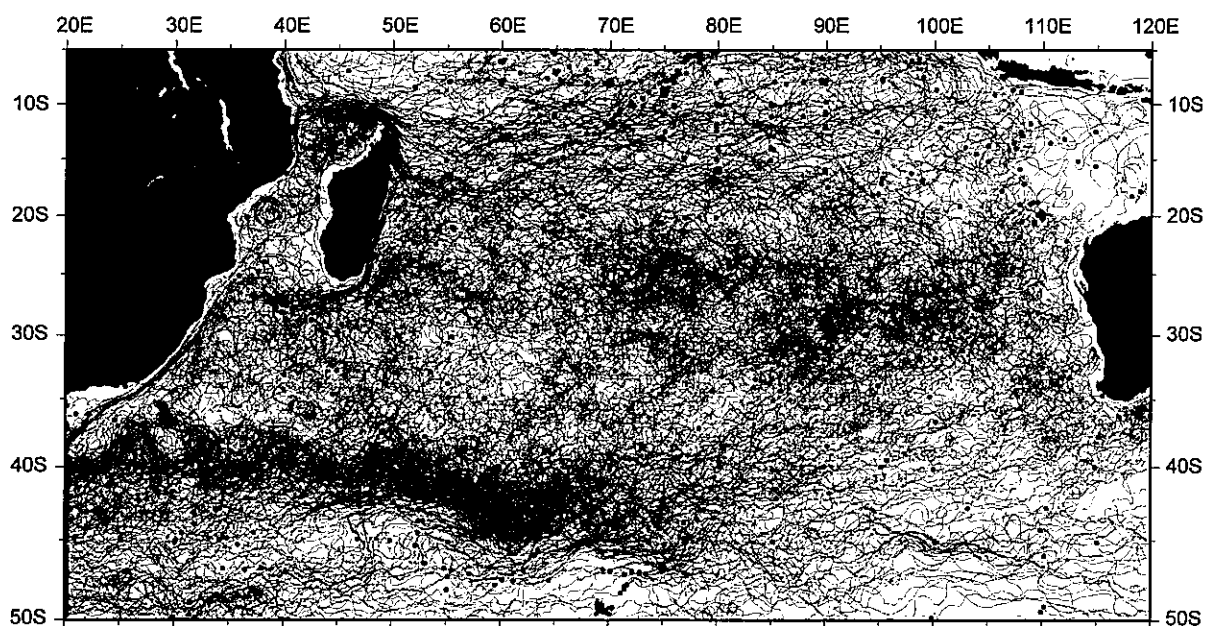


Fig. 1 Drifter trajectories (solid lines) in the south Indian Ocean (1993- 2004). Dots indicate the start positions of measurement.

Indian Ocean was analysed by Cresswell and Golding (1980)¹³⁾, Pearce and Cresswell (1985)¹⁴⁾ and Smith et al. (1991)¹⁵⁾. Recent studies of Morrow et al. (2003)¹⁶⁾ and Feng et al. (2003)¹⁷⁾ accounted the eddy circulation and the El-Nino effects on the Leeuwin Current.

Recently, the advent of satellite altimeter, which measures the sea surface height which consists of large amplitude undulations of the geoid and the small amplitude undulations of the sea surface dynamic topography. Practically, only the anomaly can be accurately determined because the present geoid model is not accurate enough for the sea surface dynamic topography to be extracted from the sea surface height. In the south Indian Ocean where there is no comprehensive in-situ observational system, altimeter data is one of the most important data streams for describing the ocean circulation. In addition, the large number of satellite tracking surface drifters deployed as a part of Global Drifter Program is still in operation and continually delivering data.

In the present study, efforts have been made to present a high resolution quantitative description of the mean circulation and the mesoscale variability of the south Indian Ocean region between 20°E and 120°E, and between 5°S and 50°S, using satellite altimeter and the satellite tracked drifter observations during the period 1993-2004. The drifters providing the more accurate, but sparse, in-situ velocity observations were used to

calibrate the satellite data, and the satellite data being more evenly sampled field in time were used to compute the mean.

2. Data and Method

The surface drifter data used in this study comes from the Global Drifter Program (Surface Velocity Program), with the positions of freely drifting buoys located using the ARGOS satellite system. The surface buoys are attached to drogues centred at 15 m depth. Data used were quality controlled and optimally interpolated to uniform six-hour interval trajectories¹⁸⁾ using the drifters' position data. This data set is compiled and maintained by the Drifter Data Centre at the Atlantic Oceanographic and Meteorological Laboratory of the National Oceanic and Atmospheric Administration, USA. The drifter tracks available for the study region during the period 1992-2004 are shown (Fig. 1).

The satellite altimeter data used in this study are Maps of Sea Level Anomaly (MSLA) produced by the Collect Localisation Satellites (CLS), France. The Maps of Sea Level Anomaly were obtained by merging JASON/ TOPEX/POSEIDON and European Remote Sensing Satellites ERS / Envisat data using optimum interpolation¹⁹⁾. Maps were produced in every seven days interval since 1992 August with a resolution of 1/3° in both Latitude and Longitude.

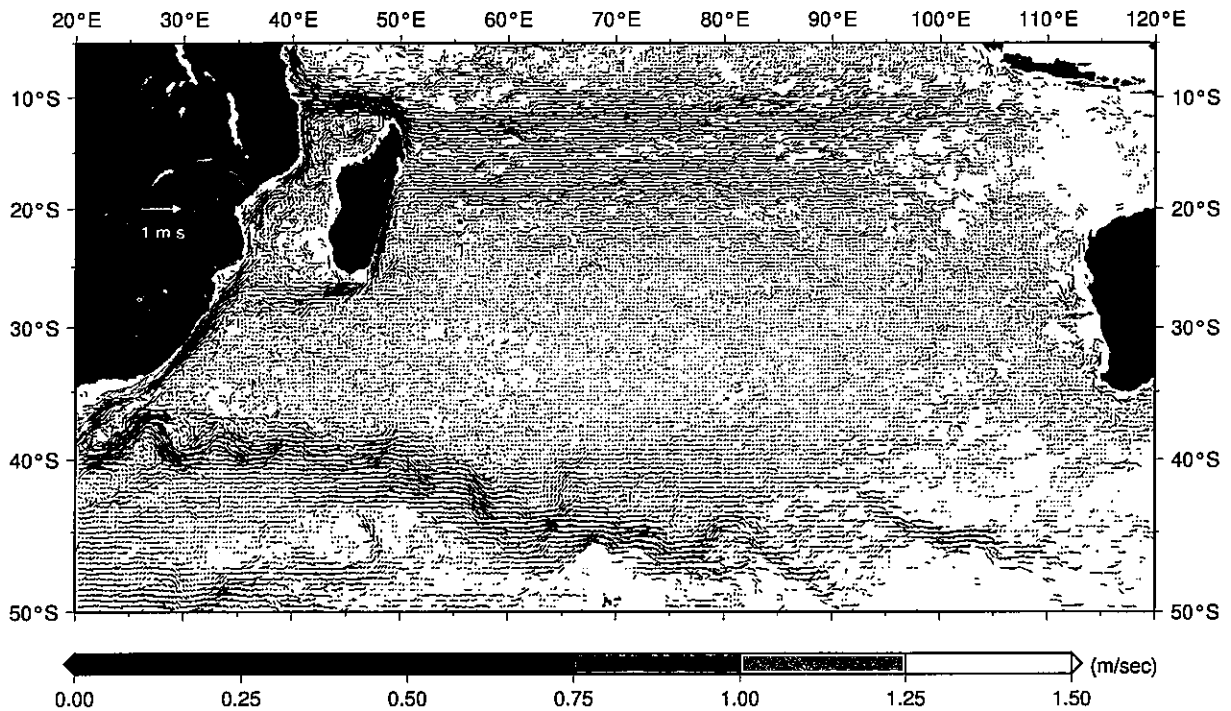


Fig. 2a Mean sea surface velocity field of south Indian Ocean estimated by combining altimetry and drifter data. Gray-scale bar indicates the scalar of vectors. The vector scale is also shown in South Africa.

The weekly ocean surface mean wind fields derived from the scatterometers onboard ERS-1/2 and Quikscat generated by CREST, France were used.

The method introduced by Uchida and Imawaki (2003)²⁰⁾ has been employed in this study, in which surface drifter and altimeter data are combined to estimate the mean surface velocity. The mean velocity is calculated by subtracting the altimeter derived geostrophic velocity anomaly from the drifter-derived geostrophic velocity measured at the same time and location. This method estimates almost unbiased Eulerian mean velocities which are free from the sampling tendency of the drifters.

At a location x and time t , the geostrophic velocity $V_g(x, t)$ can be written as

$$V_g(x, t) = V_{mg}(x) + V_g'(x, t) \quad (1),$$

where $V_{mg}(x)$ is the mean geostrophic velocity, and $V_g'(x, t)$ is the geostrophic velocity anomaly i. e.,

$$V_{mg}(x) = V_g(x, t) - V_g'(x, t) \quad (2),$$

Thus, the unknown mean velocity can be estimated for the grid box where a drifter had passed because $V_g(x, t)$ can be approximated by the drifter velocity.

The average of the calculated mean velocities in each grid, $\langle V_{mg}(x) \rangle$ gives a more accurate estimate by reducing the estimate error.

To remove the high frequency fluctuations, the drifter trajectories were low-pass filtered by a 30 hour running mean. Then, the drifter data was gridded into $1/3^\circ \times 1/3^\circ$ latitude \times longitude boxes. The surface velocity was estimated from the drifter position data. The wind-produced slip was corrected employing the relation given by Niller and Paduan (1995)²¹⁾. An additional correction was made for drifters, which had lost its drogues during its traverse, using the empirical relation given by Pazan and Niller (2001)²²⁾.

The Ekman velocity was estimated employing the Ralph and Niller (1999)²³⁾ model. The geostrophic velocity component was aparted from the drifter velocity by subtracting the Ekman component.

From the altimeter sea level anomaly data, the anomalous geostrophic velocity was computed with the conventional geostrophic relation.

$$u' = -g/f(\partial h/\partial y) \quad (3)$$

$$v' = g/f(\partial h/\partial x) \quad (4)$$

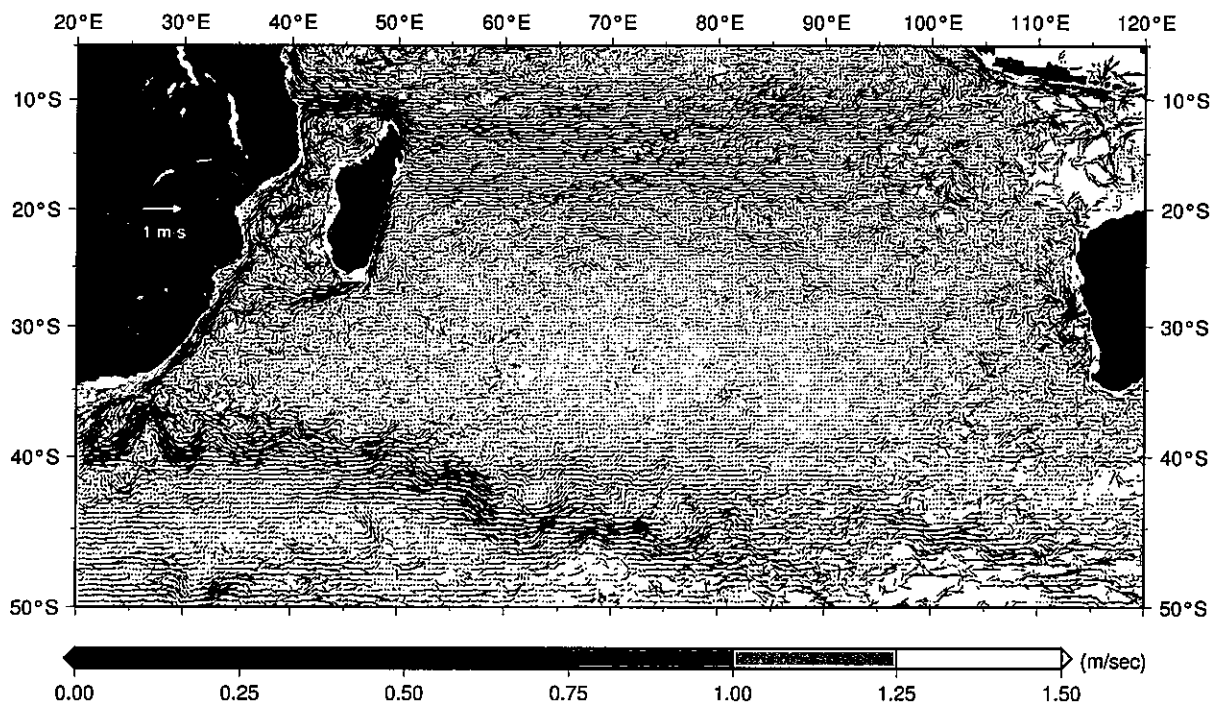


Fig. 2b Same as fig. 2a, but for simple averages of drifter-derived velocities.

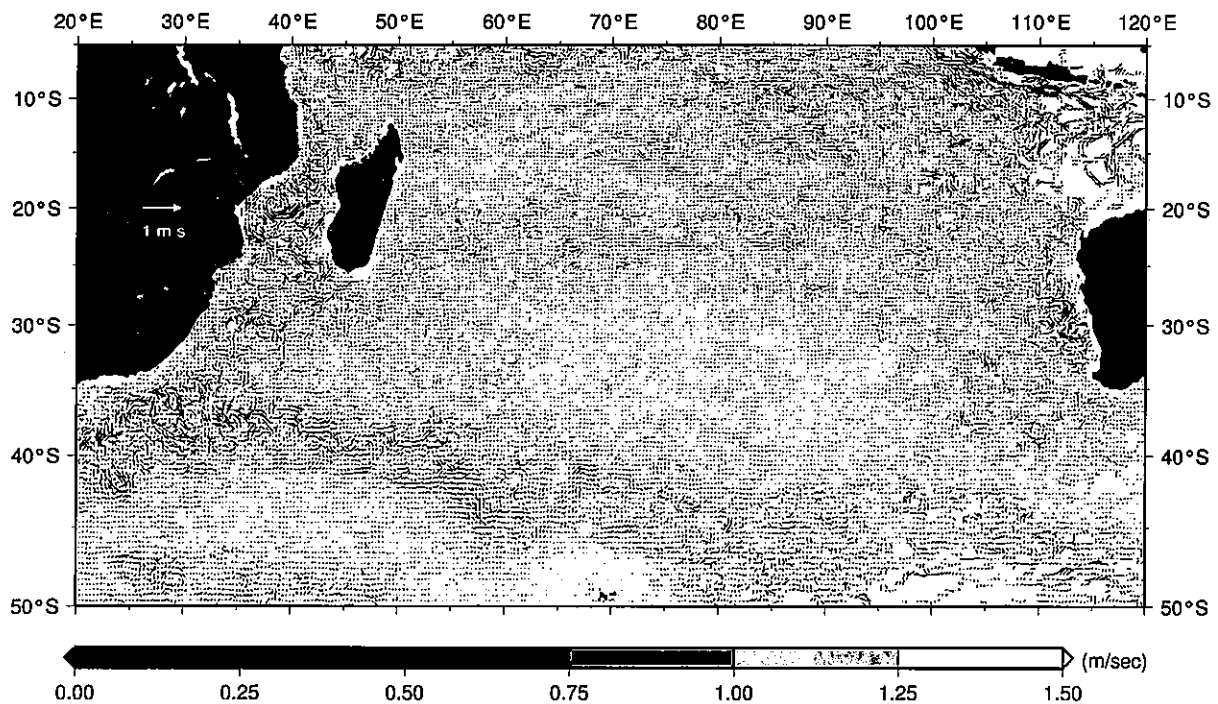


Fig. 2c Same as fig. 2a, but for averages of altimeter-derived velocities.

3. Eulerian Mean Velocity Field

The Eulerian mean velocity field obtained by combining the satellite altimeter and drifter data reveals the near surface flow pattern of the south Indian Ocean

(Fig. 2a). The altimeter derived velocity anomaly (Fig. 2c) serves as a correction to the simple averages of the drifter-derived velocities (Fig. 2b). Although the large scale flow pattern is not much different from the simple average of drifter-derived velocities, the above mentioned correction by the altimeter-derived velocity

anomaly shows significant differences along the peripherals and even above 0.5 m/s anomaly is prevailing at the Agulhas retroflexion region. The anomaly field is also prominent in the zonal flows between 5 and 15°S, and between 35 and 45°S. The Leeuwin Current and South Java Current regions also display strong anomaly field. In the following sections, we present a detailed description of the mean velocities of different current regions in the south Indian Ocean.

3a. South Equatorial Current

In the mean field, the westward flowing South Equatorial Current is prominent and is composed of two broad current cores of velocity ranging between 0.25 and 0.5 m/s. The South Equatorial Current is most persistent current in the models as well as in the real Indian Ocean²⁴⁾. The stronger core is located around 12°S and is wide whereas the second one is located along 18°S. Slightly weak flow (velocity < 0.25 m/s) occurs between these cores, which is unclear in Fig. 2b. The northern core originates even from far eastern part of the Indian Ocean and is supported by the Indonesian throughflow. The subtropical gyral circulation is feeding the southern core. Both the current cores exhibit weak velocities in the eastern part of the south Indian Ocean. The South Equatorial Current is located south of 10°S²⁵⁾ and is between 10°S and 20°S throughout the year with peak speeds reaches around 0.4 cm/s²⁶⁾.

In the northern part of the South Equatorial Current, between 5°S and 10°S, weak cyclonic eddies develop due to shear between South Equatorial Current and South Equatorial Counter Current flow. The southeast trades in the southern Indian Ocean terminate at a northern limit between 5 and 10°S. This is associated with a persistent Ekman divergence that is strongest during the summer monsoon. This region shows a conspicuous upward transport in zonally integrated stream function of several numerical models²⁷⁾. Supporting evidence for upwelling comes from satellite imagery also, which indicates the presence of phytoplankton blooms along the band²⁹⁾ and also from nutrient distribution.

3b. Western Boundary Currents

The western part of the Indian Ocean displays a powerful flow pattern. The complex topographic features, especially the Madagascar Island is much controlling the flow pattern of the southwestern Indian Ocean. The northern core of the South Equatorial

Current turns northward off the east coast of Madagascar, whereas, the southern core is flowing southward along the Madagascar Coast.

The South Equatorial Current supplies water to the North East Madagascar Current that feeds the East African Coastal Current. Very strong, broad flow is occurring along the northern tip of Madagascar where the velocity reaches even 1.5 m/s and when it impinges the east coast of Africa, branches into two flows; one is the southward flow along Mozambique Channel (Mozambique Current) and the other is the northward flow along the East African Coastal Current. Swallow et al. (1988)²⁹⁾ estimated an overall mean transport of about 30 Sv pass the northern tip of Madagascar above 1000 m, but of this only 10 Sv crosses the equator with the Somali Current³⁰⁾.

A southward Mozambique Channel throughflow of 15 ± 9 Sv was determined in the global inverse model of Ganuchand et al. (2000)³¹⁾. Powerful flow field embedded with anticyclonic eddies are occurring along the Mozambique Channel. Eddy circulation is prominent in the northern part. The anticyclonic eddies that are triggered at the northern end of the channel are arriving from the east by Rossby waves³²⁾. After passing through the channel these eddies seem to be diffused.

The East Madagascar Current advances southward along the coast and becomes a fast current as it reaches the southern tip. The major portion of this takes a southwestward turn, merges with the Mozambique Current and flow as Agulhas Current. In the southern part, the East Madagascar Current velocity reaches even up to 1.5 m/s. Also, a weak retroflexion (velocity < 0.5 m/s) occurs in the southeastern part of the Madagascar Current, when the flow slips from the land boundary. Donohue and Toole (2003)³³⁾ accounted a well-developed southward East Madagascar Current along with a strong offshore northward flow at around 14°E and 25°S. The retroflexion in the East Madagascar Current is often observed south of Madagascar³⁴⁾.

Mean velocities of even higher than 1 m/s is noticed in the major part (28-38°S) of the Agulhas Current. Africa, the western boundary of the Indian Ocean subtropical region, does not extend southward to the edge of the wind stress region, this result in the retroflexion of the Agulhas Current when it reaches the southern end of Africa, distinguishing the Agulhas from the subtropical western boundary currents of the other oceans. While the Agulhas Current reaches 40°S it executes an abrupt anticyclonic turn and feeds water into the eastward flowing Agulhas Return Current. The retroflexion develops strong eddy recirculation and meandering flow towards east. The major part of the

eastward flow is merging with the Circumpolar Current at 70°E and 45°S, near the Kerguelen plateau region whereas; a minor portion joins the subtropical gyral circulation. The Agulhas Current, the strongest western boundary current in the southern hemisphere oceans, the mean velocity even reaches above 1.5 m/s. Earlier transport estimates of Agulhas Current vary between 9 Sv and 136 Sv³⁴⁾. Recently, Beal and Bryden (1999)³⁵⁾ estimated the transport as 75 Sv using LADCP. From year-long current measurements of the Agulhas Current, the long-term mean transport is obtained as 70 Sv.

3c. Eastern Boundary Currents and South Java Current

Mean velocity field is weak in the southeastern part of the Indian Ocean. The poleward flow (Leeuwin Current) along the west coast of Australia is faintly visible in the north; between 20 and 25°S, velocities around 0.5 m/s are noticed. But, between 25 and 32°S the southward flow is much disturbed and weak eddy circulation is apparent. Beyond 32°S again southward flow prevails and it turns towards the South Pacific Ocean along the southwestern tip of Australia. The mean velocity field is not exhibiting a continuous streamlined poleward flow of the Leeuwin Current, instead weak eddies are embedded in the flow field. An average of six long-lived warm core eddies are generated per year³⁶⁾. The seasonal weakening of the Leeuwin Current is clear from observations⁶⁾. The current is strong during southern autumn and winter and appears to be weakening by about November^{14) 37)}.

South off Java, a strong southeastward flow prevails and the mean velocity exceeds even 1 m/s near the Lombok Strait. Thus, the mean field depicts the southeastward flow of the South Java Current. The South Java Current is recognized as a seasonal reversing current that reverses to southeastward flow semi-annually around May and November, probably through the propagation of coastal and equatorial Kelvin waves forced by westerly wind bursts during the monsoon transitions in the equatorial Indian Ocean. During these times, the South Java Current has been found to consist of narrow cores of accelerated flow extending to depths of 150 m – 200 m and 90 m south of Java to 10°S and the boundary with westward flowing South Equatorial Current^{38) 39)}.

4. Comparison with ADCP Data

Using the time series of altimeter-derived velocity

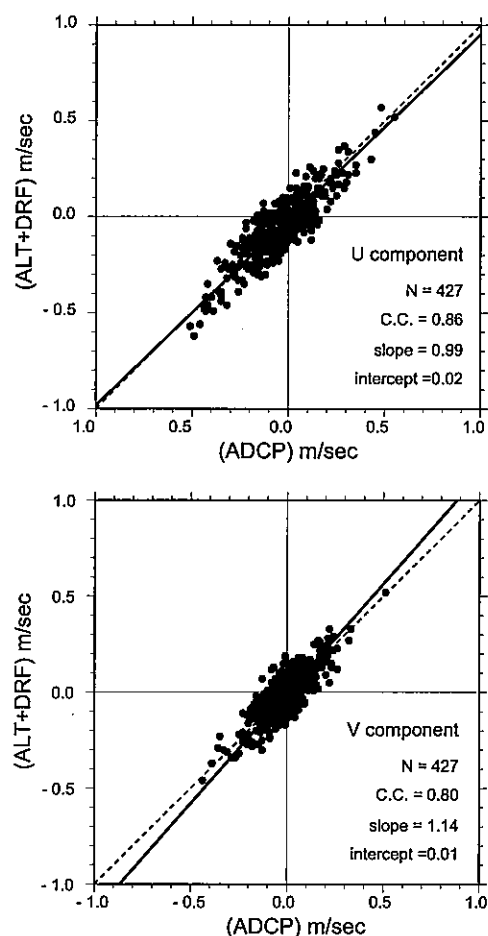


Fig. 3 Scatter plot of estimated instantaneous surface velocity components (ordinate) against ADCP- derived surface velocity components (abscissa).

anomaly field and the estimated Eulerian mean velocity field, we computed the instantaneous velocity field every seven days to compare with the available in-situ velocities measured by shipboard Acoustic Doppler Current Profiler (ADCP) data obtained from the WOCE cruises (WOCE Global Data version 3.0). The depth of ADCP data used varies from 20-30 m and we assume that it represent the near surface geostrophic current. The instantaneous velocity estimated in this study is in good agreement with the ADCP derived velocities (Fig. 3). The fitted regression lines are close to unity (0.99 and 1.14 for the u and v velocity components, respectively), and have very high correlation co-efficients of 0.86 and 0.80, respectively.

5. Summary

The mean velocity field estimated by combining the satellite altimetry and drifter observations confirms

the general flow pattern of south Indian Ocean and bring out the details of magnitude of various currents in the region. The anticyclonic gyral circulation is characterised by strong southward western boundary currents and very weak eastern boundary currents. The zonal westward flow of the South Equatorial Current is comparatively strong and broad, and exhibits double-core structure. The zonal eastward flows is very powerful and meandering in the south. Strong currents prevails in the northern, western and southern parts whereas, the central and eastern parts exhibit dull circulation (velocity < 0.25 m/s). The Agulhas Current is the strongest current in the south Indian Ocean and its mean speed even reaches above 1.5 m/s. The Agulhas retroflection region characterized by the recirculation eddy and the strong meandering eastward flow is conspicuous in the mean field. The southward flowing Leeuwin Current (eastern boundary current) is not obvious in the mean field. But, strong southeastward flow is observed south off Java.

Acknowledgements

This work was supported by Japan Society for Promotion of Sciences under the long-term invitation fellowship programme. We used altimeter data set produced by the Collect Localisation Satellites, Space Oceanography Division as part of Environment and Climate. Drifter data provided by the National Oceanic and Atmospheric Administration, Atlantic Oceanographic and Meteorological Laboratory were utilized. Also employed the wind data set produced and provided by the French Processing and Archiving Facility (CERSAT) at the French Research Institute for Exploration of the Sea. The ADCP data used were from the WOCE data products.

References

- 1) Wyrтки, K.: Oceanographic Atlas of the International Indian Ocean Expedition, National Science Foundation, Washington, 531p (1971).
- 2) Reverdin, G., M. Fieux, J. Gonella and J. Luyten: Free drifting buoy measurements in the Indian Ocean equatorial jet, in Hydrodynamics of Equatorial Ocean, J. C. H. Nihoul, ed., Elsevier, NY, 99-120 (1983).
- 3) Shetye, S. R., and G. S. Michael: Satellite-tracked drifting buoy observations in the south equatorial current in the Indian Ocean, Proc. Indian Acad. Sci. (Earth and Planet.), 97, 149 -157 (1988).
- 4) Molinari, R. L., D. Olson and G. Reverdin: Surface current distributions in the tropical Indian Ocean derived from compilations of surface buoy trajectories, J. Geophys. Res., 95, 7217- 7238 (1990).
- 5) Shenoi, S. S. C., P. K. Saji, and A. M. Almeida: Near surface circulation and kinetic energy in the tropical Indian Ocean derived from Lagrangian drifters, J. Mar. Res., 57, 885-907 (1999).
- 6) Benny, N. P. and K. Mizuno: Annual cycle of steric height in the Indian Ocean estimated from the thermal field. Deep-Sea Res., Part 1, 47, 1351-1368 (2000).
- 7) Reid, J. L.: On the total geostrophic circulation of the Indian Ocean: Flow patterns, tracers, and transports, Progr. Oceanogr., 56(1), 137-186 (2003).
- 8) Woodberry, K. E., M. E. Luther, and J. J. O'Brien: The wind driven seasonal circulation in the southern tropical Indian Ocean, J. Geophys. Res., 94, 17985-18002 (1989).
- 9) Kindle, J. C., and J. D. Thompson: The 20- and 50-day oscillations in the Western Indian Ocean: model results, J. Geophys. Res., 94, 4721-4736 (1989).
- 10) Grundlingh, M. L.: Drift observations from Nimbus VI –Satellite tracked buoys in the South western Indian Ocean, Deep-Sea Res., 24, 903 -913 (1997).
- 11) Stramma, L., and J. R. E. Lutjeharms: The flow field of the subtropical gyre of the South Indian Ocean, J. Geophys. Res., 102, 5513-5530 (1997).
- 12) Bryden, H. L., and L. M. Beal: Role of the Agulhas Current in the Indian Ocean circulation and associated heat and freshwater fluxes, Deep-Sea Res., Part 1, 48, 1821-1845 (2001).
- 13) Cresswell, G. R., and J. J. Golding: Observations of a south-flowing current in the southeast Indian Ocean. Deep-Sea Res., 27A, 449 -466 (1980).
- 14) Pearce, A. F. and G. R. Cresswell: Ocean circulation off western Australia and Leeuwin Current, CSIRO Inf. Sheety, 16-3, 4pp (1985).
- 15) Smith, R. L., A. Huyer, J. S. Godfrey, and J. A. Church: The Leeuwin Current off western Australia. J. Phys. Oceanogr., 21, 323 – 345 (1991).
- 16) Morrow, R., F. Fang, M. Fieux, and R. Molcard: Anatomy of three warm-core Leeuwin Current eddies, Deep-Sea Res. II, 50, 2229-2243 (2003).
- 17) Feng, M., G. Meyers, A. Pearce, and S. Wijffels: Annual and interannual variations of the Leeuwin current at 32°S, J. Geophys. Res., vol.108, C11, 3355 (2003).
- 18) Hansen, D. V., and P. M., Poulain: Quality control and interpolations of of WOCE-TOGA drifter data,

- J. Atmos. Oceanic Technol., 13, 900-909 (1996).
- 19) Archiving, Validation, and Interpretation of Satellite Oceanographic Data (AVISO), AVISO Handbook: Sea Level Anomaly Files, 21st ed., 24 pp. (1997).
 - 20) Uchida, H., and S. Imawaki: Eulerian mean surface velocity field derived by combining drifter and satellite altimeter data, *Geophys. Res. Lett.*, Vol. 30 (5), 1229 (2003), DOI:10.1029/2002GLO16445
 - 21) Niiler, P. P. and D. Paduan: Wind-driven motions in the northeast Pacific as measured by Lagrangian drifters, *J. Phys. Oceanogr.*, 25, 2819-2830 (1995).
 - 22) Pazan, S. E., and P. P., Niiler: Recovery of near surface velocity from undrogued drifters, *J. Atmos. Oceanic Technol.*, 18, 476-479 (2001).
 - 23) Ralph, A. E and P. P. Niiler: Wind-driven currents in the tropical Pacific, *J. Phys. Oceanogr.*, 29, 2121-2129 (1999).
 - 24) Jensen, T.: Equatorial variability and resonance in a wind-driven Indian Ocean model, *J. Geophys. Res.*, 98, 22533-23552 (1993).
 - 25) Hastenrath, S., and L. Greischar: The monsoonal current regimes of the tropical Indian Ocean: observed surface flow fields and their geostrophic and wind-driven components. *J. Geophys. Res.*, 96, 12619 – 12633 (1991).
 - 26) Haugen, V. E., O. M. Johannessen and G. Evensen: Indian Ocean: Validation of the Miami Isopycnic Coordinate Ocean Model and ENSO events during 1958 – 1998, *J. Geophys. Res.*, 107, 101029-101057 (2002).
 - 27) Gartnericht, U., and F. Schott: Heat fluxes of the Indian Ocean from a global eddy- resolving model, *J. Geophys. Res.*, 102, 21147-21159 (1997).
 - 28) Muttugudde, R., S. Signorini, J. Christian, A. Busalacchi, C. McClain, and J. Picaut: Ocean color variability of the tropical Indo-Pacific basin observed by SeaWiFS during 1997-98, *J. Geophys. Res.*, 104 18351-18366 (1999).
 - 29) Swallow, J. C., M. Fieux, and F. Schott: The boundary currents east and north of Madagascar, Part I: Geostrophic currents and transports, *J. Geophys. Res.*, 93, 4951-4962 (1988).
 - 30) Schott, F., J. C. Swallow, and M. Fieux: The Somali Current at the equator: annual cycle of currents and transports in the upper 1000 m and connection to neighboring latitudes, *Deep-Sea Res.*, 37, 1825-1848 (1990).
 - 31) Ganachaud, A., C. Wunsch and Marotzke: The meridional overturning and large-scale circulation of the Indian Ocean, *J. Geophys. Res.*, 105, 26117-26134 (2000).
 - 32) De Ruijter, W. P. M., H. Ridderinkhof, J. R. E. Lutjeharms, and M. W. Schouten: Direct observations of the flow in the Mozambique Channel, *Geophys. Res. Lett.*, 29, 140.1-140.3 (2002).
 - 33) Donohue, K. A., and J. M. Toole: A near synoptic survey of the Southwest Indian Ocean, *Deep-sea Res.*, Part II, 50, 1893-1931 (2003).
 - 34) Lutjeharms, J.: Remote sensing corroboration of retroflection of the East Madagascar Current. *Deep-Sea Res.*, Part 1, 35, 2045-2050 (1988).
 - 35) Beal, L., and H. Bryden: The velocity and vorticity structure of the Agulhas Current at 32°S, *J. Geophys. Res.*, 104(C3), 5151-5176 (1999).
 - 36) Grundlingh, M. L.: On the volume transport of the Agulhas Current; *Deep-Sea Res.*, Part 1, 27, 557-563 (1980).
 - 37) Feng, F., and R. Morrow: Evolution and structure of Leeuwin Current eddies in 1995-2000, *Deep-Sea Res.*, Part 1, 2245-2261 (2002).
 - 38) Benny, N. P., P. Sreeraj, and K. G. Vimalkumar: Structure and variability of the Leeuwin Current in the south eastern Indian Ocean, *J. Indian Geophysical Union*, 9, 107-119 (2005).
 - 39) Fieux, M., C. Andrie, P. Delecluse, A. G. Ilahude, A. Kartavtseff, F. Mantsi, R. Molcard, and J. C. Swallow: Measurements within the Pacific-Indian oceans throughflow region. *Deep-Sea Res.*, Part 1, 41, 1091-1130 (1994).
 - 40) Meyers, G., R. J. Bailey, and A. P. Worby: Geostrophic transport of Indonesian Throughflow, *Deep-Sea Res.*, Part 1, 42, 1163-1174, (1995).